Original Article

New approaches to improve a WCDMA SIR estimator by employing different post-processing stages

Amnart Chaichoet and Chalie Charoenlarpnopparut*

*Electronics and Communication Engineering Program, School of Communications, Instrumentations and Control,
Sirindhorn International Institute of Technology, Thammasat University
Khlong Luang, Pathum Thani, 12121 Thailand.*

Abstract

For effective control of transmission power in WCDMA mobile systems, a good estimate of signal-to-interference ratio (SIR) is needed. Conventionally, an adaptive SIR estimator employs a moving average (MA) filter (Yoon *et al.*, 2002) to encounter fading channel distortion. However, the resulting estimate seems to have high estimation error due to fluctuation in the channel variation. In this paper, an additional post-processing stage is proposed to improve the estimation accuracy by reducing the variation of the estimate. Four variations of post-processing stages, namely 1) a moving average (MA) post-filter, 2) an exponential moving average (EMA) post-filter, 3) an IIR post-filter and 4) least-mean-squared (LMS) adaptive post-filter, are proposed and their optimal performance in terms of root-mean-square error (RMSE) are then compared by simulation. The results show the best comparable performance when the MA and LMS post-filter are used. However, the MA post-filter requires a lookup table of filter order for optimal performance at different channel conditions, while the LMS post-filter can be used conveniently without a lookup table.

Keywords: conventional SIR estimator, adjustable SIR estimator, W-CDMA, moving average filter, exponential moving average filter, LMS algorithm, multi-path fading, Doppler frequency, transmission power control

1. Introduction

Interference levels in WCDMA systems need to be controlled to an optimal level since they can effect the cell user capacity as well as the quality of service. One of the key features of WCDMA systems, under 3GPP standard, is the power control capability. As the mobile station moves away from the connecting base station, the signal power-to-interference power ratio (SIR) gradually decreases and results in a poor quality of service. On the other hand, as the mobile station moves toward the base station, the SIR gradually increases which may result in an unnecessarily strong transmission power (becoming interference to other users). To remedy this problem, a power control scheme is employed to adjust, via a feedback control loop, the transmission power level of the mobile station to be in an optimal range based on the estimated value of SIR. This accurate estimation of SIR is crucial to the effectiveness of the power control principle. Traditionally, the SIR estimator employs only the correlator and simple fixed-length moving average filter (Yoon *et al.*, 2002). Later, the adjustable-length moving average filter was proposed (Charoenlarpnopparut *et al.*, 2004). In this paper, an SIR estimator with four variations of post-processing stages, namely 1) a moving average (MA) post-filter, 2) an exponential moving average (EMA) post-filter, 3) an IIR post-filter and 4) least-mean-squared (LMS) adaptive post-filter, are studied and their optimal performance are then compared.

The organization of this paper is as follows. First, the development of the SIR estimator is explained. Then, in the main section, the proposed post-processing stages to improve

*Corresponding author.
  Email address: chalie@siit.tu.ac.th

the estimation accuracy are described. Before the conclusion, the simulation results obtained from using different post-processing schemes are compared.

2. Background of SIR Estimator Development

SIR stands for signal-to-interference-ratio; the SIR estimator is the algorithm which is used to estimate the ratio of the power between the transmitted signal and the interference signal. It is important to the power control process because the transmit power control (TPC) can be more effective with a more accurate SIR measurement.

2.1 Conventional SIR Estimator

The conventional scheme, as shown in Figure 1, estimates SIR by averaging the received pilot symbols over a fixed interval of one slot, corresponding to 0.667 ms regardless of the channel condition, where the pilot symbols in the dedicated physical channel (DPCH) are used for estimating the channel condition. The instantaneous interference component can be obtained by removing the estimated signal from the received signal. The amount of the interference power is estimated by averaging the instantaneous interference over a few slots. Each finger of the rake receiver in the WCDMA system needs an SIR estimator. We assume that the multi-path channel has L resolvable paths and that there are no path losses and ignore shadowing effects for ease of description. Since the SIR estimator is connected to the rake receiver, which has l fingers in a typical mobile phone, therefore, the received signal of the kth slot from the lth path of the nth symbol after despreading can be written as (Yoon et $al.$, 2002):

$$r_l[n,k] = h_l[n,k]p[n,k] + z_l[n,k], \qquad (1)$$

where n is the symbol sequence $\in \{0, 1, ..., 7\}$, $h_l[n,k]$ is the complex channel gain (impulse response) of the nth symbol in the kth slot, $p[n,k]$ is the pilot sequence and $z_l[n,k]$ is the sum of the background noise and Multiple Access Interference (MAI) including the interference from other paths.

Next the received signal is duplicated and separated into two parts; one is used for calculating the power of the

signal in terms of channel impulse response, and the other is used for calculating the power of the interference. Since the pilot sequence is a complex signal, to find the power of the signal, the channel impulse response is found by multiplying the complex conjugate of that pilot sequence with the received signal and the estimated impulse response from l^{th} path in k^{th} slot can be expressed as:

$$\hat{h}_l[k] = \frac{1}{N_p} \sum_{n \in T_p} r_l[n,k] p^*[n,k], \qquad (2)$$

$$= h_l[k] + \frac{1}{N_p} z_l[k], \qquad (3)$$

where N_p is the number of symbols in T_p and T_p is the field of the pilot symbol in the DPCH sequence (3GPP, 2002).

Therefore, by taking the square of the magnitude, the signal power $\hat{S}_l[k]$ of the kth slot in the lth path can be represented as:

$$\hat{S}_l[k] = |\hat{h}_l[k]|^2 . \qquad (4)$$

Also, after the estimated channel impulse response, $\hat{h}_l[k]$, is found, the estimated channel gain, $\hat{h}_l[k]p[n,k]$, is used to estimate the instantaneous interference in the kth slot from the lth path by subtracting the estimated channel gain from the received signal $r_l[n,k]$ as follows:

$$I_l[k] = r_l[n,k] - \hat{h}_l[k]p[n,k]. \qquad (5)$$

From the magnitude squared, the interference power $\overline{I}_l[k]$ in k^{th} slot can be expressed as:

$$\overline{I}_l[k] = \frac{1}{N_p} \sum_{n \in T_p} |I_l[k]|^2, \qquad (6)$$

$$= \frac{1}{N_p} \sum_{n \in T_p} |r_l[n,k] - \hat{h}_l[k]p[n,k]|^2 . \qquad (7)$$

To cancel any unexpected noise, a 1-pole IIR filter, which has a low pass characteristic, is used at the final stage. The output of the low pass filter can be expressed as:

$$\hat{I}_l[k] = \alpha \hat{I}_l[k-1] + (1-\alpha)\hat{I}_l[k], \qquad (8)$$

where α is the pole of the IIR filter. Finally, the power ratio between signal and interference can be written as:
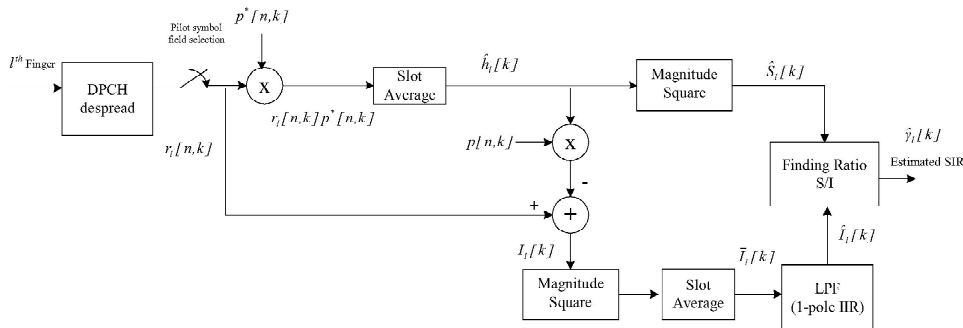

Figure 1. Conventional SIR Estimator

$$\hat{\gamma}_l[k] = \frac{\hat{S}_l[k]}{\hat{I}_l[k]}. \qquad (9)$$

2.2 Adjustable SIR Estimator

When the channel has slow multipath fading, there is strong correlation between the signals in the adjacent slots. As a result, in (Yoon *et al.*, 2002), it may be possible to obtain an improved SIR estimate by considering the signals in the adjacent slots. Since the channel condition is time varying, it is desirable to adjust the number of slots for SIR estimation in response to the channel condition.

The adjustable SIR estimate scheme, as shown in Figure 2, considers the use of previous $\hat{h}_l[k]$ depending on the channel condition parameters obtained by the channel condition estimator. To optimally combine the precious channel gains, it may be desirable to employ a low pass filter whose coefficients are adjustable according to the channel condition. For ease of design, the moving average (MA) filter, whose tap size N is adjusted depending upon the channel condition, is considered. The estimate of the channel impulse response in k^{th} slot can be calculated by:

$$\bar{h}_{l,N}[k] = \frac{1}{N}\sum_{j=1}^{N}\hat{h}_l[k-(j-1)], \qquad (10)$$

$$= \frac{1}{N}\frac{1}{N_p}\sum_{j=1}^{N}\sum_{n\in T_p}\{\hat{h}_l[n,k-(j-1)] + z_l[n,k-(j-1)]\}, \qquad (11)$$

$$= h_l[k] + \frac{1}{N}\frac{1}{N_p}z_l[k], \qquad (12)$$

where N is the tap size of the MA filter. Then, the signal power is estimated as:

$$\hat{S}_l[k] = |\bar{h}_{l,N}[k]|^2 . \qquad (13)$$

And the instantaneous interference of the kth slot can be represented by:

$$I_l[k] = \frac{1}{N_p}\sum_{n\in T_p}|r_l[n,k] - \bar{h}_{l,N}[k]p[n,k]|^2 . \qquad (14)$$

3. Improving Performance by adding Post-processing stage

A post-processing stage is proposed for reducing the fluctuation of the estimated SIR with respect to the channel condition (Doppler frequency or equivalently the velocity of the mobile phone). From Figure 3 the received signal $r_l[n,k]$ is separated to the SIR estimator and velocity estimator. The algorithm of an adjustable SIR estimator is already shown in Figure 2. The velocity estimator is used to estimate the Doppler frequency f_d and then send it through the look up table to find the suitable value of tap size N for the SIR estimator and suitable values for parameter(s) for the post-processing stage depending on the type of filter. Table 1 shows the parameter(s) used for each filter.

In this paper, four additional variations of the post processing stages are proposed and compared, namely:

- SIR estimator with a moving average (MA) post-filter
- SIR estimator with an exponential moving average (EMA) post-filter
- SIR estimator with an IIR post-filter
- SIR estimator with least-mean-squared (LMS) adaptive post-filter

3.1 Moving Average (MA) Filter

The block diagram of the MA filter (Charoenlarpnopparut *et al.*, 2004) is shown in Figure 4. This filter is a noncausal filter with odd window size W and makes use of the estimated SIR, $\hat{\gamma}_l[k]$, according to the changing channel. Therefore, the new SIR of the lth path can be esti-

Table 1. Parameters used in each filter

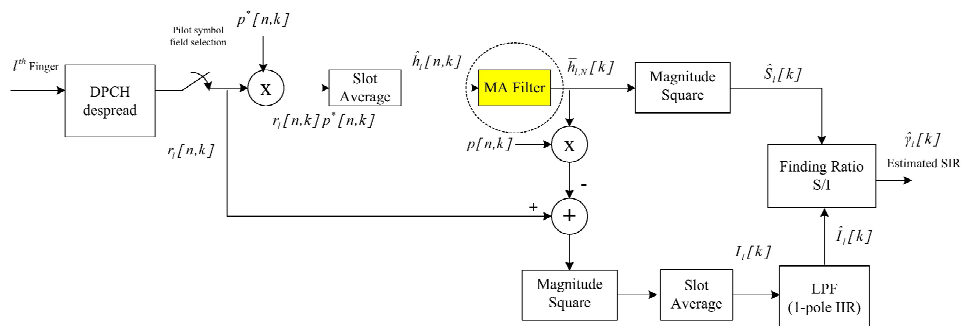| Type of filter	Parameter(s)
MA	window size (W)
EMA	weight parameter (w)
IIR	filter coefficients (order & cutoff frequency)
LMS	step size (μ)

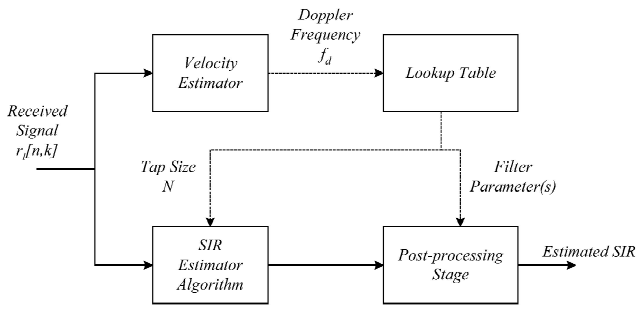Figure 2. Adjustable SIR Estimator

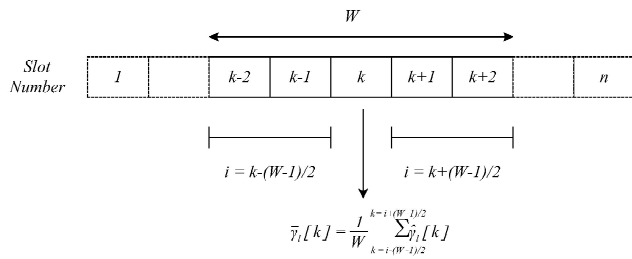Figure 3. Post-processing Scheme
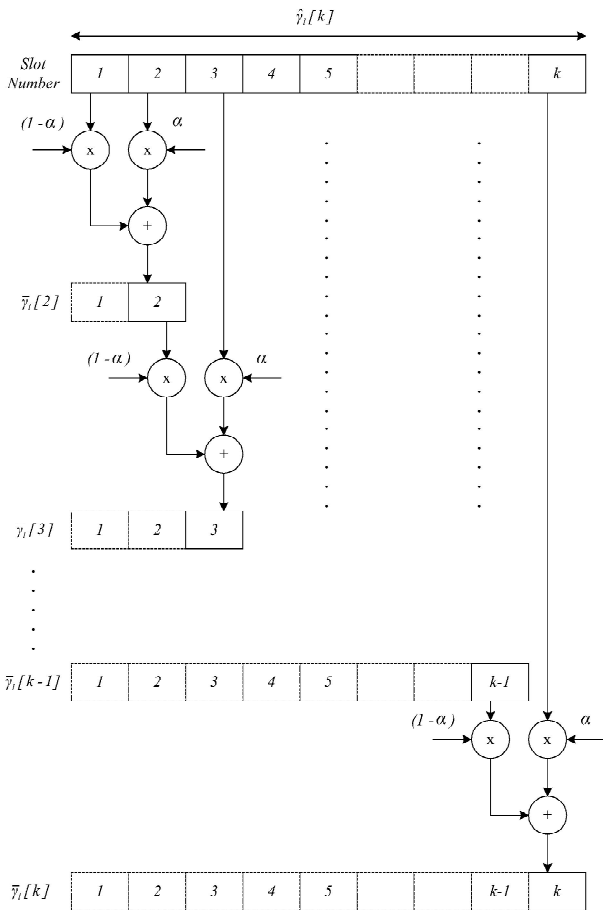

Figure 4. The Structure of MA Filter

Figure 5. The Structure of EMA Filter

mated as:

$$\bar{\gamma}_l[k] = \frac{1}{W}\sum_{k=i-\frac{W-1}{2}}^{k=i+\frac{W-1}{2}} \hat{\gamma}_l[k], \quad \forall i, \tag{15}$$

and

$$\bar{\gamma}_l[k] = \hat{\gamma}_l[k], \text{ for } k \leq \frac{W-1}{2}, \tag{16}$$

where k is the slot number, and W is the window size of the MA filter.

3.2 Exponential Moving Average (EMA) Filter

The second way to improve the SIR values is by applying an exponential moving average (EMA) filter (Chaichoet *et al.*, 2005) instead of the noncausal MA filter. The block diagram of this scheme is represented in Figure 5 and the new estimated SIR can be written as:

$$\bar{\gamma}_l[k] = \beta\hat{\gamma}_l[k] + (1-\beta)\bar{\gamma}_l[k-1], \text{ for } k > 1, \tag{17}$$

and

$$\bar{\gamma}_l[k] = \hat{\gamma}_l[k], \text{ for } k = 1, \tag{18}$$

where $\beta = \dfrac{2}{w+1}$, and w is the weight parameter.

3.3 IIR Filters

Another possibility to improve the SIR values is to make use of the IIR filter (Chaichoet *et al.*, 2005), in this paper, two types of IIR filters namely, a Chebyshev filter, and a Butterworth filter are used at the post-processing stage instead of the two algorithms presented above.

The transmission functions for Chebyshev filters (Type I) of even and odd order are shown in Eq.(19)-(20). The Chebyshev filter exhibits an equiripple response in the passband and a monotonically decreasing transmission in the stopband. All the transmission zeros of the Chebyshev filter are at $\omega = \infty$, making it an all-pole filter.

The magnitude of the transfer function of an Mth order Chebyshev filter with a passband edge (ripple bandwidth) is given by:

$$|T(j\omega)| = \frac{1}{\sqrt{1+\epsilon^2 \cos^2[M\cos^{-1}(\omega/\omega_p)]}}, \text{ for } \omega \leq \omega_p, \tag{19}$$

and

$$|T(j\omega)| = \frac{1}{\sqrt{1+\epsilon^2 \cosh^2[M\cosh^{-1}(\omega/\omega_p)]}}, \text{ for } \omega \geq \omega_p. \tag{20}$$

At the passband edge, $\omega = \omega_p$, the magnitude function is given by:

$$|T(j\omega_p)| = \frac{1}{\sqrt{1+\epsilon^2}}. \tag{21}$$

Thus, the parameter ε determines the passband ripple according to:

$$A_{max} = 10\log(1+\epsilon^2),\qquad (22)$$

Conversely, given A_{max}, the value of ε is determined from:

$$\epsilon = \sqrt{10^{A_{max}/10}-1}.\qquad (23)$$

The attenuation achieved by the Chebyshev filter at the stopband edge ($\omega = \omega_s$) is found using Eq.(19) as

$$A(\omega_s) = 10\log[1+\epsilon^2\cosh^2(M\cosh^{-1}(\omega_s/\omega_p))].\ (24)$$

With the aid of a calculator, this equation can be used to determine the minimum order M required to obtain a specified A_{min} by finding the lowest integer value of M that yields $A(\omega_s) \geq A_{min}$. As in the case of the Butterworth filter, increasing the order M of the Chebyshev filter causes its magnitude function to approach the ideal brick-wall low-pass response. Finally, the poles of the Chebyshev filter are given by:

$$p_k = -\omega_p\sin(\frac{2k-1}{M}\frac{\pi}{2})\sinh(\frac{1}{M}\sinh^{-1}\frac{1}{\epsilon}) + j\omega_p\cos(\frac{2k-1}{M}\frac{\pi}{2})\cosh(\frac{1}{M}\sinh^{-1}\frac{1}{\epsilon}),$$
$$(25)$$

for $k = 1, 2, …, M$.

Therefore, the transfer function of the Chebyshev filter can be written as:

$$T(s) = \frac{K}{(s-p_1)(s-p_2)\cdots(s-p_M)},\qquad (26)$$

where K is chosen to satisfy the desired dc gain of the filter.

Next is the Butterworth filter; this filter exhibits a monotonically decreasing transmission with all transmission zeros at $\omega = \infty$, making it an all-pole filter. The magnitude function for an Mth order Butterworth filter with a passband edge ω_p is given by:

$$|T(j\omega)| = \frac{1}{\sqrt{1+\epsilon^2(\frac{\omega}{\omega_p})^{2M}}}.\qquad (27)$$

At $\omega = \omega_p$

$$|T(j\omega_p)| = \frac{1}{\sqrt{1+\epsilon^2}}.\qquad (28)$$

Thus, the parameter ε determines the maximum variation in passband transmission, A_{max}, according to:

$$A_{max} = 20\log\sqrt{1+\epsilon^2},\qquad (29)$$

Conversely, given A_{max}, the value of can be determined from:

$$\epsilon = \sqrt{10^{A_{max}/10}-1}.\qquad (30)$$

Observe that in the Butterworth response the maximum deviation in passband transmission (from the ideal value of unity) occurs at the passband edge only. It can be shown that the first $2M - 1$ derivatives of $|T|$ relative to ω are zero at $\omega = 0$. This property makes the Butterworth response

very flat near and gives the response the name *"maximally flat"* response. The degree of passband flatness increases as the order M is increased, and as the order M is increased the filter response approaches the ideal brick-wall type response.

At the edge of the stopband, $\omega = \omega_s$, the attenuation of the Butterworth filter is given by:

$$A(\omega_s) = -20\log[1/\sqrt{1+\epsilon^2(\omega_s/\omega_p)^{2M}}],\qquad (31)$$

$$= 10\log[1+\epsilon^2(\omega_s/\omega_p)^{2M}].\qquad (32)$$

This equation can be used to determine the filter order required, which is the lowest integer value of M that yields $A(\omega_s) = A_{min}$. Then, the transfer function can be written as:

$$T(s) = \frac{K_0\omega_c^M}{(s-p_1)(s-p_2)...(s-p_M)},\qquad (33)$$

where K_0 is also a constant equal to the required dc gain of the filter, ω_c is the -3dB cutoff frequency, and p_k, $k = 1, 2, …, M$ are the poles of the Butterworth filter distributed equally in the LHP on the circle with radius ω_c.

3.4 Least-Mean-Squared (LMS) Adaptive Filter

Adaptive filters are digital filters capable of self-adjustment. These filters can change in accordance to their input signals. Its operation relies on a recursive algorithm which makes it possible for the filter to perform satisfactorily in environments where complete knowledge of the relevant signal characteristics is not available. According to these intelligent characteristics of the adaptive filter, the adaptive filter requires two inputs which are the input signal $x(n)$ and the desired signal $d(n)$.

An adaptive filter has the ability to update its coefficients. New coefficients are sent to the filter from a coefficient generator. The coefficient generator is an algorithm that modifies the coefficient in response to an incoming signal.

As shown from Figure 6, the block diagram of an adaptive filter model, the unknown system is modeled by an FIR filter with adjustable coefficients. Both the unknown system and the FIR filter are excited by an input signal $x(n)$. The adaptive filter output $y(n)$ is compared with desired response $d(n)$ to produce the error signal $e(n)$. The error signal represents the difference between the unknown system output and the model output. The error $e(n)$ is then used as the input to an adaptive control algorithm, which corrects the individual tap weight of the filter. This process is repeated through several iterations until the error signal $e(n)$ becomes sufficiently small.

The least-mean-squared (LMS) adaptive algorithm (Chaichoet *et al.*, 2005) is a linear filtering algorithm that consists of two basic processes:

1. A Filtering Process: This process involves:
    (a) Computing the output of a linear filter in response to an input signal.
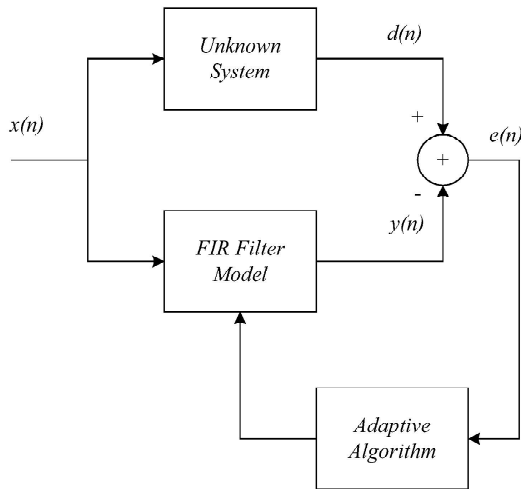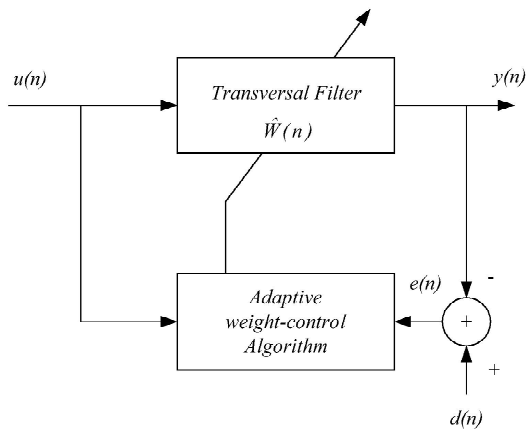
Figure 6. System Identification Model

Figure 7. Block Diagram of Adaptive Transversal Filter

(b) Generating an estimation error by comparing this output with a desired response.

2. An Adaptive Process: This process involves the automatic adjustment of the parameters of the filter in accordance with the estimation error.

The combination of these two processes constitute a feedback loop, as illustrated in Figure 7. First, the LMS filter is built around a transverse filter; this component is responsible for performing the filtering process. Then, the mechanism for performing the adaptive control process on the tap weights of the transversal filter is used.

Details of the transversal filter component are presented in Figure 8. The tap inputs $u(n)$, $u(n-1)$, ..., $u(n-M+1)$ form the elements of the $M - by - 1$ tap-input vector $u(n)$, where $M-1$ is the number of delay elements. Correspondingly, the tap weights $\hat{w}_0(n), \hat{w}_1(n),...,\hat{w}_{M-1}(n)$ form the elements of the $M - by - 1$ tap-weight vector $\hat{\mathbf{w}}(\mathbf{n})$.

The value computed for this vector using the LMS algorithm represents an estimate whose expected value may come close to the Wiener solution $\mathbf{W_0}$, for a wide-sense
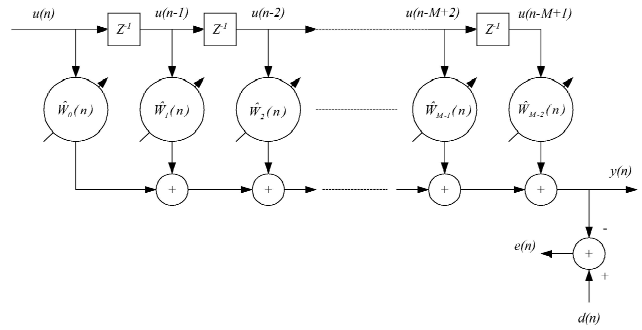

Figure 8. Detailed Structure of the Transversal Filter Component

stationary environment, as the number of iterations n approaches infinity.

During the filtering process, the desired response $d(n)$ is supplied for processing, alongside the tap-input vector $u(n)$. Given this input, the transversal filter produces an output $y(n)$ used as an estimate of the desired response $d(n)$. Accordingly, we may define as estimate error $e(n)$ as the difference between the desired response and the actual filter output, as indicated in the output at the end of Figure 8. The estimation error $e(n)$ and the tap-input vector $u(n)$ are applied to the control mechanism, and the feedback loop around the tap weights is thereby closed.

Figure 9 presents details of the adaptive weight-control mechanism. Specifically, a scalar version of the inner product of the estimation error $e(n)$ and the tap input $u(n-k)$ is computed for $k = 0$, 1, 2, ..., $M-2$, $M-1$. The obtained result defines the correction $\delta\hat{w}_k(n)$ applied to the tap weight $\hat{w}_k(n)$ at iteration $n+1$. The scaling factor used in this com-
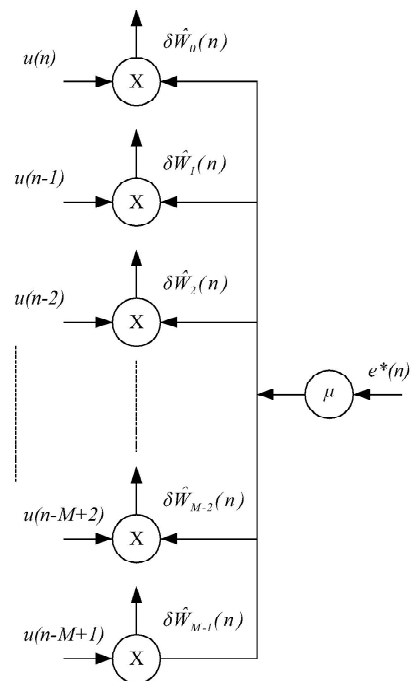

Figure 9. The Structure of the Adaptive Weight Control Mechanism

putation is denoted by a positive quantity μ in Figure 10 called the step-size parameter. To conserve the stability, an important criterion is required.

$$J(n) \rightarrow J(\infty) \text{ as } n \rightarrow \infty, \quad (34)$$

where $J(n)$ is the mean-square error produced by the LMS filter at time n and its final value $J(\infty)$ is a constant. An algorithm that satisfies this requirement is said to be stable in the mean square. For the LMS algorithm to satisfy this criterion, the step-size parameter μ has to satisfy a certain condition related to the spectral content of the tap inputs.

If the input vector $\boldsymbol{u}(\boldsymbol{n})$ and the design response $d(n)$ are jointly stationary, the cost function, $J(n)$, at time n is written by using the definitions of the correlation **R** and the cross-correlation vector **p** as:

$$J(n) = \sigma^2 - w^H(n)\mathbf{p} - \mathbf{p}^H w(n) + w^H(n)\mathbf{R}w(n). \quad (35)$$

To develop an estimate of the gradient vector $\nabla J(n)$ at each iteration n, the most obvious strategy is to substitute estimates of the correlation matrix **R** and the cross-correlation vector **p**, which can be expressed by:

$$\nabla J(n) = -2\mathbf{p} + 2\mathbf{R}w(n). \quad (36)$$

Instantaneous estimates for **R** and **p** are the simplest choice of estimators, which are based on sample values of the tap-input vector and desired response, defined by:

$$\mathbf{R}(n) = \mathbf{u}(n)\mathbf{u}^H(n), \quad (37)$$

and

$$\hat{\mathbf{p}}(n) = \mathbf{u}(n)d^*(n). \quad (38)$$

An exact estimate of the gradient vector $\nabla J(n)$ at each iteration n and suitable step-size parameter μ are needed in computing the optimum tap-weight vector, $\hat{\mathbf{w}}(\mathbf{n})$. Therefore, the instantaneous estimate of the gradient vector is:

$$\hat{\nabla} J(n) = -2\mathbf{u}(n)d^*(n) + 2\mathbf{u}(n)\mathbf{u}^H(n)\widehat{\mathbf{w}}(n). \quad (39)$$

However, this estimate is biased, because the tap-weight estimate vector $\hat{\mathbf{w}}(\mathbf{n})$ depends on the tap-input vector $\boldsymbol{u}(\boldsymbol{n})$.

Therefore, the result in the form of three basic relations can be expressed as follows:

1. Filter output:

$$y(n) = \widehat{\mathbf{w}}^H(n)\mathbf{u}(n). \quad (40)$$

2. Estimation error or error signal:

$$e(n) = d(n) - y(n). \quad (41)$$

3. Tap-weight adaptation:

$$\widehat{\mathbf{w}}(n+1) = \widehat{\mathbf{w}}(n) + \mu\mathbf{u}(n)e^*(n). \quad (42)$$

Equations (40)-(41) define the computation of the estimation error $e(n)$ which is based on the current estimate of tap-weight vector $\hat{w}(n)$. The term $\mu u(n)e^*(n)$ is considered as the adjustment that is applied to $\hat{w}(n)$, where its initial condition is set to be $\hat{w}(0)$. The algorithm, described by Eqs.(40) - (42), is the complex form of the adaptive LMS algorithm. Knowledge of the most recent values (e.g. $u(n)$,
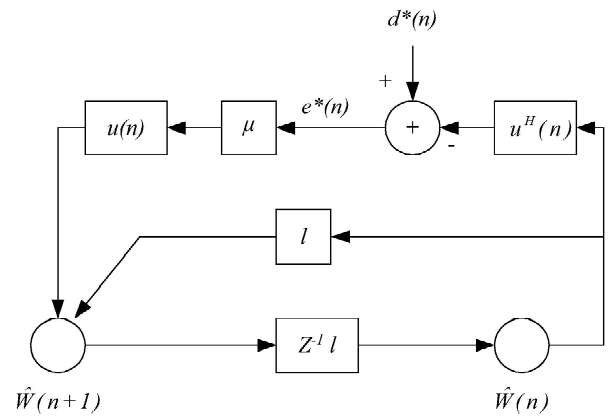

Figure 10. Signal flow graph representation of LMS algorithm

$d(n)$, and) is required for this algorithm at each time update. A representation of signal flow of the LMS algorithm in the form of a feedback model is shown in Figure 10, where the simplicity of the LMS algorithm is illustrated. From Figure 10, the LMS algorithm requires only *2M+1* complex multiplications and *2M* complex additions per iteration. *M* is the number of tap weights used in the adaptive transversal filter. Since the instantaneous estimates of **R** and **p** are used in the algorithm, the LMS algorithm seems to be incapable of performing well at first sight. During the course of adaption, these estimates are averaged effectively because the LMS algorithm is recursive in nature.

4. Simulations and Performance Comparisons

In these simulations, using MATLAB, the suitable window size *W* for the MA filter, the optimal weight parameter *w* for EMA filter, the filter coefficients for IIR filter, and the step-size parameter μ for LMS adaptive algorithm are found by searching and minimizing the mean-square-error (MSE).

It is noted that the performance of all schemes are evaluated by using computer simulation with the following input parameters shown in Table 2 following 3GPP specification (TS 25.101, and TS 25.111).

The time-varying characteristics of the channel are mostly effected by the Doppler frequency, which is directly related to the speed and can be expressed as

$$f_d = vf_c / c, \quad (43)$$

Table 2. Input Parameters

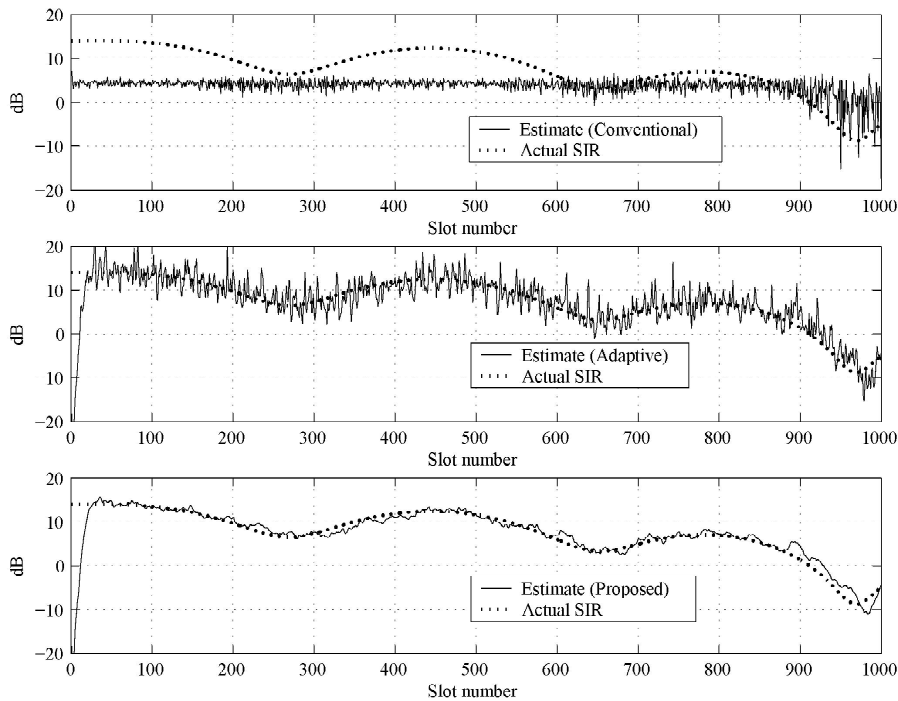|	
Carrier Frequency (f_c)	2 GHz
Pilot bits per Slot (N_p)	4
Doppler Frequency (f_d)	0 - 250 Hz
Channel Model	ITU Vehicular A
AWGN	-12 dB

Figure 11. The plots of estimated SIR vs the actual SIR using (top) conventional scheme, (middle) adjustable (adaptive) scheme and (bottom) adjustable (adaptive) scheme with MA post-filtering

where f_d is the Doppler frequency, f_c is the carrier frequency, c and v are the speed of light and the mobile station, respectively.

Since the performance of the system directly depends on noise and mobile speed (doppler frequency) when the signal is transmitted through the channel, it is assumed that AWGN at -12 dB is the worst case for noise in the system while mobile speeds are varied (0 - 135 km/hr). The performance of the new SIR estimators are measured in terms of root-mean-square error (RMSE).

The channel is assumed to have only one signal path to simplify simulation. The performances of the three SIR estimate schemes, namely, the conventional SIR estimator, the adjustable (adaptive) SIR estimator, and the SIR estimator with post-processing scheme are depicted in Figure 11.

Figure 11 (TOP) shows the performance of the conventional SIR scheme and it shows that the trend of the estimated SIR does not follow the actual SIR. With the adaptive scheme, Figure 11 (MIDDLE), the trend of the estimated SIR follows the actual SIR but a high level of noise is apparent. To improve the result of the system, post-processing with a MA filter Figure 11 (BOTTOM) is applied.

Figure 12 compares the performances of the adaptive SIR schemes, i.e. the adaptive scheme without the post-processing filter, and the adaptive scheme with different filters. It is shown that the adaptive SIR estimator with a post-processing scheme gives better performance than without the scheme. It is also shown that at low Doppler frequency, e.g. $f_d = 10$ Hz, the performances of EMA post-

filtering and IIR post-filtering are almost the same. On the other hand, Figure 13 shows that the EMA post-filtering performs better than the IIR post-filtering in case of high Doppler frequency, e.g. $f_d = 150$ Hz, and these 2 filters are recommended in case of real-time implementation because of low complexity. Note that the ripple for IIR filters is considered at 0.1 dB.

For the LMS algorithm, the adaptive filter is dependent on an input vector $\boldsymbol{u}(\boldsymbol{n})$ and the desired response $d(n)$
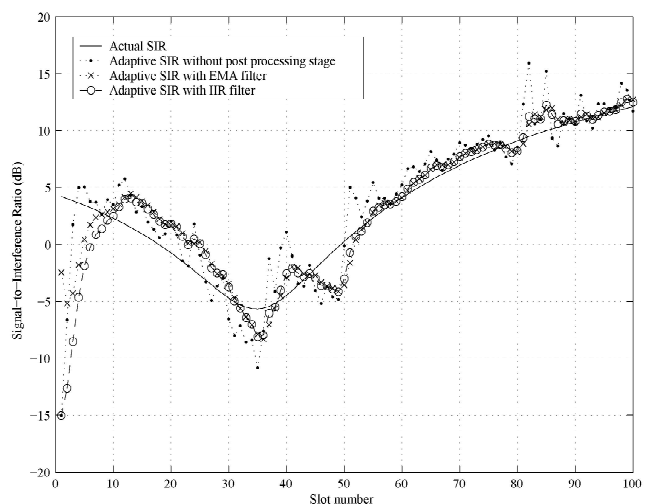

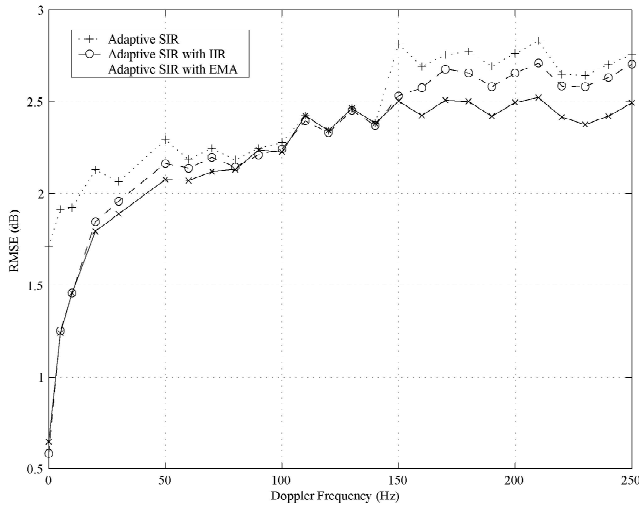Figure 12. Signal-to-Interference Ratio vs slot number for Doppler frequency $f_d = 10$ Hz and tap size $N = 4$

Figure 13. RMSE vs f_d of an Adjustable (adaptive) SIR with and without post-processing stage

to produce a minimum mean-square error (MMSE), which is adjustable by varying the filter length M. The LMS adaptive filter coefficient (e.g. Tap-weight, w) is updated until the optimal value that provides the minimum RMSE is obtained. The step-size parameter μ is suitably chosen to obtain the optimum tap-weight vector provided in Table 6.

In a real environment, where complete knowledge of the characteristics of the desired signal is not available, the delay of the input vector $\boldsymbol{u(n-1)}$ is replaced and used in the computation of the error estimation $\boldsymbol{e(n)}$ by comparing

to the output $\boldsymbol{y(n)}$. After getting the optimal tap-weight w, the estimated SIR is obtained from the direct calculation.

Figure 14 compares the performances of two schemes, i.e. (a) the adjustable (adaptive) estimation scheme and (b) the LMS adaptive estimation scheme, over 1500 slots under interference and additive white Gaussian noise (AWGN). The obtained SIR estimation of both LMS adaptive schemes provide large fluctuations over the first 500 slot numbers. This is a result of the tap-weight adaptation where time is needed to converge to an optimal value since the tap-weight vector was first set to be zero.

The actual implementation of the lookup tables is shown as follows: Table 3 summarizes the effect of the Doppler frequency on the tap size of the first MA filter in the adjustable SIR estimator, and the sub-optimal window size, W, used in the second MA filter at the post-processing stage. Table 4 summarizes the effect of the Doppler frequency on the weight parameter, w. Table 5 summarizes the effect of the Doppler frequency on the optimal filter coefficients of IIR filter (Butterworth), and Table 6 summarizes the effect of the Doppler frequency on the optimal step-size parameter, μ.

5. Conclusion

The conventional SIR estimator estimates the SIR by averaging the received pilot symbols over a fixed interval of one slot regardless of the channel condition. While the adjustable SIR estimator improves the estimation by considering the signals in the adjacent slots; it is desirable that the number of slots is adjusted in response to the channel condi-
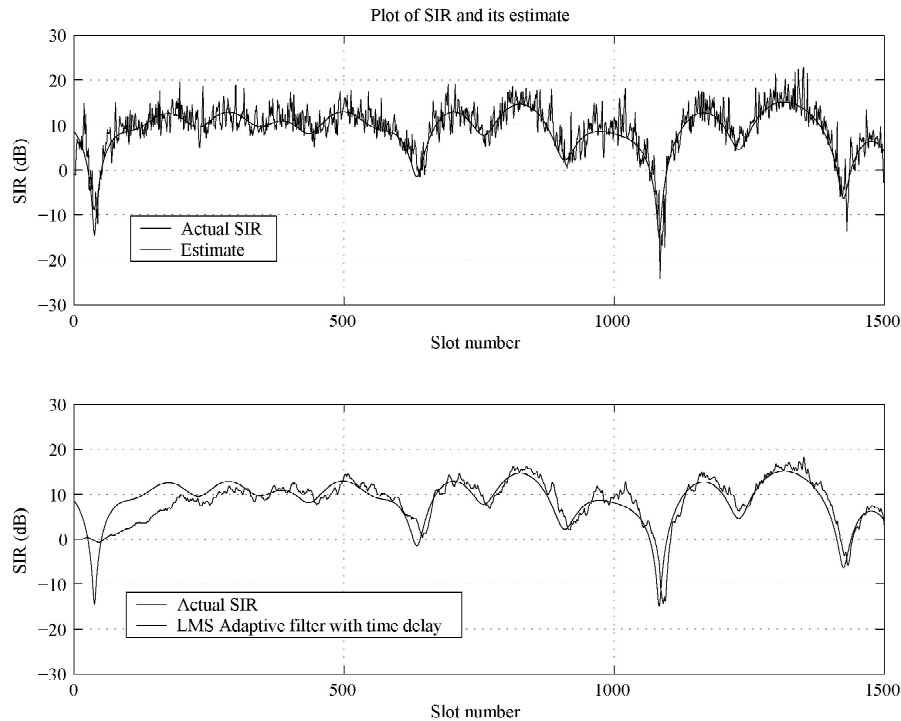

Figure 14. SIR Estimated by (a) Adjustable (adaptive) SIR estimator, (b) LMS Adaptive estimator

Table 3. Lookup Table for MA Filter

Doppler Frequency (f_d)	Optimal Tap Size (N)	Optimal Window Size (W)	Minimum RMSE (dB)
0	20	159	0.8437
5	20	61	1.1060
10	8	45	1.2340
20	8	27	1.3140
30	6	17	1.6748
50	5	15	1.7841
60	5	15	1.6843
70	4	11	1.8218
80	4	9	1.9344
90	4	11	1.9611
100	3	9	2.1012
110	3	9	1.9593
120	3	9	2.0234
130	3	7	2.1232
140	3	7	1.9945
150	3	7	2.1237
160	3	7	2.1991
170	3	7	2.2795
180	3	7	2.2048
190	3	7	2.4185
200	3	5	2.4668
210	2	5	2.4722
220	3	7	2.4166
230	2	5	2.5269
240	2	5	2.3558
250	2	5	2.4749

Table 4. Lookup Table for EMA Filter

Doppler Frequency (f_d)	Optimal Tap Size (N)	Optimal Window Size (w)	Minimum RMSE (dB)
0	7	39	1.480
5	6	12	3.046
10	6	13	3.175
20	4	7	4.882
30	5	5	4.626
50	4	4	6.067
60	4	5	5.718
70	3	4	6.977
80	3	3	7.387
90	3	3	7.465
100	3	3	7.030
110	3	3	7.901
120	3	3	8.176
130	3	2	9.065
140	3	2	8.777
150	3	2	8.437
160	3	2	8.863
170	2	2	8.872
180	2	2	9.095
190	2	2	9.531
200	2	2	9.540
210	2	2	9.944
220	2	2	9.277
230	2	2	9.389
240	2	2	10.500
250	2	2	9.988

tion. At the post-processing stage, a filter is applied to further smooth out the estimation error.

The adjustable SIR estimator scheme with post-processing stage has been presented as an alternative to the estimation of SIR in WCDMA mobile systems. It has been proposed on ground tests that it could improve the estimation accuracy because it can provide a much smoother estimate and thus a large reduction of the estimation error and the root mean square error. It is noted that the averaging is done in the post-processing stage and the tap size N has to be considered after adding any filters.

- Moving Average Filter: This non-causal FIR filter, whose window size, W, can be adjusted according to the channel condition, gives the best performance among all filters presented here. The disadvantage is that it must use one filter per channel.

- Exponential Moving Average Filter: This kind of causal filter depends on the weight parameter, w. It has the worst performance among the filters presented here and it also must use one filter per channel, like the MA filter. The advantage is that it has the lowest complexity, so it is easier to implement the hardware.

- IIR Filters: The performance of these filters depends greatly on the selection of filter coefficients (e.g. order and normalized cut-off frequency). From the simulations and the lookup tables, the most suitable orders, M, for all of the IIR filters are low in order (i.e. 1st order or 2nd order). For each IIR filter, the minimum root mean square values are almost the same (see Table 5), for the sake of convenience, therefore, the Butterworth filter is used and presented. It performs better than the EMA filter, but worse than the MA filter and LMS filter. The optimization of the IIR filter depends on the channel condition, so a lookup table is required.

- Least-Mean-Squared Adaptive Filter: After studying the possibility of using an adaptive filter for SIR approximation, the results show that an adaptive filter has rather the same efficiency in estimating the value of the signal-to-interference ratio (SIR). Actually, the errors produced from estimating SIR by using an adaptive filter are nearly equal to those produced by the moving average filter at the optimum window size. At low Doppler frequency, the RMSE produced from the adaptive filter is slightly lower than that produced from the moving average filter. The RMSE increases as filter length, M, decreases. The main advantages of the LMS

Table 6. Lookup Table for LMS Adaptive Filter

Doppler Frequency (f_d)	Optimal Tap Size (N)	Optimal Window Size (μ)	Minimum RMSE (dB)
0	20	0.00000620	1.4146
30	20	0.00001405	2.3370
50	5	0.00001560	2.7200
60	5	0.00001310	2.6297
70	4	0.00001900	2.9180
80	4	0.00002215	3.0217
90	4	0.00001920	3.0350
100	3	0.00001910	2.9700
110	3	0.00002080	3.1620
120	3	0.00001820	3.1944
130	3	0.00002010	3.4236
140	3	0.00002000	3.4415
150	3	0.00002450	3.3461
160	3	0.00002030	3.4546
170	3	0.00002040	3.6976
180	3	0.00002070	3.8390
190	3	0.00002000	3.8602
200	3	0.00001510	3.5952
210	2	0.00001300	3.6856
220	3	0.00001800	4.1402
230	2	0.00001500	3.6515
240	2	0.00001200	3.3935
250	2	0.00001090	3.8625

Table 5. Lookup Table for Butterworth Filter

Doppler Frequency (f_d)	Optimal Tap Size (N)	Order (X)	Normalized Cut-Off Frequency	Minimum RMSE (dB)
0	18	1	0.011	0.583
50	2	1	0.409	2.163
100	2	1	0.9	2.280
150	2	1	0.9	2.539

algorithm are, 1) Simplicity of implementation, 2) Robust performance, 3) Small μ, slow convergence, small steady-state excess RMSE. Finally, an adaptive filter has many significant advantages over a moving average filter, such as low computational complexity, and the ability of adapting itself to a changing environment without having to re-enter any parameters. For the LMS adaptive filter, a lookup table is not needed. Only one filter is needed for all channel conditions.

References

Bose, N.K. 1993. DIGITAL FILTERS: Theory and Applications, Krieger Publishing Company, Florida.

Chaichoet, A., Charoenlarpnopparut, C., Prompijit, A., Palungvitvatana, K., and Nualplaud, N. 2005. Approaches to Improve WCDMA Adaptive SIR Estimator by LMS Algorithm and IIR Post-filtering, Proceedings of the 2005 Electrical Engineering/Electronics, Computer, Telecommunications, and Information Technology (ECTI) International Conference (ECTI-CON 2005), 12-13 May, 2005, Pattaya, Thailand, pp. 434-437.

Charoenlarpnopparut, C., Clungnooch, C., and Rosjan, C. 2004. Improved Adaptive W-CDMA SIR Estimator with Post-Processing, Proceedings of the First Electrical Engineering/Electronics, Computer, Telecommunications, and Information Technology (ECTI-CON 2004) Annual Conference, 13-14 May, 2004, Pattaya, Thailand, pp. 50-53.

Gong, Y., Boroujeny, B.F., and Lim, T.J. 2001. Variable Step-Size LMS Blind CDMA Multiuser Detector, 2001 IEEE International Conference on Acoustics Speech and Signal Processing, Salt Lake City.

Holm, H., and Toskala, A. 2001. WCDMA of UMTS: Radio Access for Third Generation Mobile Communications, Wiley.

Sedra and Smith, Microelectronic Circuits, International Fourth Edition, Oxford, pp. 892-899.

Seo, S., Dohi, T., and Adachi, F. 1998. SIR-Based Transmit Power Control of Reverse Link for Coherent DS-CDMA Mobile Radio, IEICE Trans. Commun., Vol. E-81, No. 7, 1998, pp. 1508-1516.

Simon Haykin, Adaptive Filter Theory, International Edition, Prince Hall, pp. 1-13, 101-141.

Yoon, Y-S., and Lee, Y-H. 2002. Adaptive SIR Estimation in WCDMA Systems, Vehicular Technology Conference, 2002. VTC Spring 2002. IEEE, 55, Vol. 1, 2002, pp. 275-279.

3GPP. 2002. 3G Specification Note TS 25.111 – Physical channel and mapping of transport channels onto physical channels, http://www.3gpp.org/specs/specs.html

3GPP. 2001. 3G Specification Note TS 25.101 - UE Radio transmission and reception (FDD), http://www.3gpp.org/specs/specs.html